ARCADE OF MAGNETIC LINES PASSING THROUGH THE CHAIN OF DENSITY MAXIMA: THE RESULT OF MHD SIMULATION ABOVE ACTIVE REGION IN ORDER TO OBTAIN CONDITIONS FOR ACCELERATION OF SOLAR COSMIC RAYS

A. I. Podgorny[1, *] and I. M. Podgorny[2, **]

[1]*Lebedev Physical Institute of the Russian Academy of Sciences, Moscow 119991, Russia*

[2]*Institute of Astronomy of the Russian Academy of Sciences, Moscow 119017, Russia*

In order to study the physical mechanism of solar cosmic ray acceleration, it is necessary to simultaneously study the physical mechanism of a solar flare and the physical mechanism of charged particle acceleration, since solar cosmic rays are generated during solar flares. Appearance of the solar flare is explained by the physical mechanism based on the accumulation of energy in the magnetic field of the current sheet formed in the vicinity of a singular line of magnetic field. The fast release of magnetic energy of the current sheet leads to the observed manifestations of a flare, which are explained by the electrodynamic model of a solar flare proposed by I. M. Podgorny. Generation of solar cosmic rays occurs as a result of acceleration of charged particles by the induction electric field, which is equal to the field $\mathbf{V}\times\mathbf{B}/c$ near the current sheet. Since it is impossible to obtain the magnetic field configuration in the corona from observations, it is necessary to carry out MHD simulation above the active region.MHD simulation will also allow us to obtain the configurations of the electric and magnetic fields to study the acceleration of cosmic rays. The problem of the coincidence of the flare positions found from the MHD simulation results with the observed flare positions can be solved by the appearance of a surface of increased current density passing through a chain of current density maxima. It is the surface of magnetic lines which have the form of arcade. The flare can appear due to instability which is initiated at the top of the arcade, where the current density maxima do not appear, but the field configuration has properties that best promote the appearance of flare instability.

1. INTRODUCTION

Solar cosmic rays (SCRs) are generated at fast release of magnetic energy during solar flares. Therefore, in order to understand the physical mechanism of SCR generation (in particular, in order to later be able to predict the appearance of SCRs based on understanding the physical mechanism of their generation), it is necessary to study simultaneously the physical mechanism of a solar flare and the physical mechanism of charged particle acceleration during an explosive flare process.

SCRs reach the spacecraft where they are recorded within a period of time after the appearance of a flare, from 20 minutes to several hours, depending on the conditions of their propagation in the solar wind.

Not all flares are accompanied by the appearance of solar cosmic rays. Only 30% of the most powerful flares (class X) cause the appearance of SCR. According to our ideas, charged particles are always accelerated at the site of the primordialre release of energy in the solar corona, but they will not always be able to escape from the magnetic field configuration above the active region.

Primordial energy release of the solar flare takes place in the solar corona at the altitude 15 000 km - 70 000 km (1/40 - 1/70 of the Solar radius). of this is the appearance of a source of flare thermal X-ray emission on the limb ([1]). This also follows from numerous observations and their analysis (see for example [2–4] and is confirmed by the results of numerical MHD simulation above the active region ([5–7]).

The appearance of flare high in the corona is explained by the solar flare mechanism, according to which, the energy accumulated in the magnetic field of the current sheet is released [8, 9]. A current sheet is created in the vicinity of the X-type singular line of magnetic field as a result of plasma movement under the influence of magnetic forces $\mathbf{j}\times\mathbf{B}/c$. During the process of qasi-stationary evolution, the current sheet transfers into an unstable state. The instability leads to the explosive release of the magnetic energy of the sheet with observable manifestations of the flare, which are explained by the electrodynamic model of the solar flare proposed by I. M. Podgorny [10]. The force of magnetic tension along the sheet accelerates, first of all, electrons that carry electric current. The Hall electric field $\mathbf{j}\times\mathbf{B}/nec$

* Electronic address: podgorny@lebedev.ru

** Electronic address: podgorny@inasan.ru

, resulting from the appeared charge separation, generates an electric current circuit of two field-aligned currents along magnetic lines exiting from the current sheet, which are closed by the Petersen current on the photosphere. Electrons accelerated in field-aligned currents produce beam hard X-ray emission with energies of 50-100 keV (and higher) in the lower dense layers of the solar atmosphere. electrodynamic model of solar flare uses analogies with the electrodynamic model of substorm, previously proposed by its author based on measurements on the "Intercosmos-Bulgaria-1300" spacecraft [11].

An important consequence of the explosive process in the current sheet is the generation of solar cosmic rays. The induced electric field in the current sheet, caused by a rapid change in the magnetic field during flare instability, equal to the field $\mathbf{V}\times\mathbf{B}/c$ near the current sheet, leads to the acceleration of solar cosmic rays, mainly protons, to energies of 20 GeV. I. M. Podgorny noted that this process of generating solar cosmic rays is the implementation of a more general mechanism of acceleration of charged particles in the plasma at the site of the appearance of a powerful current by the electric field causing this current, equal to the field $\mathbf{V}\times\mathbf{B}/c$ near this current [12, 13].

Another example of this mechanism at work are the processes in a laboratory experiment, carried out to solve the problem of controlled thermonuclear fusion. Particle acceleration occurs in a pinch during rapid compression of plasma by a magnetic field of a rapidly increasing electric discharge current [14].

Since it is impossible to obtain the configuration of the magnetic field in the corona from observations, to study the flare situation it is necessary to carry out MHD simulations in the solar corona. When setting the problem, no assumptions were made about the mechanism of the solar flare. All conditions were taken from observations. The problem was set to determine the mechanism of a solar flare from the results of numerical MHD simulation. To study the physical mechanism of a solar flare, calculations must begin several days before the flare, when magnetic energy for the flare has not yet accumulated in the corona.

The electric and magnetic fields obtained by MHD simulation above a real active region at the site of the primordial flare energy release and near it are necessary for studying the generation of solar cosmic rays. The acceleration of charged particles and the possibility of particles exit from the acceleration region to be studied by calculating the trajectories of charged particles in electric and magnetic fields obtained by MHD simulation. The first results of studying the acceleration of charged particles were obtained by calculating tra-

jectories in electric and magnetic fields found by MHD simulation above the active region under simplified conditions [15]

The magnetic field configurations in the corona obtained by MHD simulation are quite complex. In the places of flares, additional fields can be superimposed on the X-type field, which greatly complicates the search for the position of a singular line directly from the calculated magnetic field. For this purpose, a graphical system for search for flare positions has been developed, which, as its application has shown, has facilitated the solution of the task. However, further research indicates the necessity to improve this search system.

To further study the mechanism of solar cosmic ray acceleration, it is necessary to more accurately determine the flare positions in the real magnetic field, where the situation is complicated by the superposition of additional fields on the X-type field. It is also necessary to determine the magnetic field configuration at the flare location in the existing complex conditions well enough. The present study is aimed at finding magnetic field configurations in which magnetic energy for solar flare can accumulate, and also at more accurately determining the fields at the solar flare location, which can be used to study the acceleration of solar cosmic rays.

2. SETTING OF THE PROBLEM AND DEVELOPED NUMERICAL METHODS

MHD simulation is carried out above the active region AR 10365 during the time interval from 24.05.2003 20:48 to 27.05.2003 20:48. The computational domain in the corona is a rectangular parallelepiped ($0 \leq x \leq 1$, $0 \leq y \leq 0.3$, $0 \leq z \leq 1$) (the length unit was chosen $L_0 = 4 \times 10^{10}$ cm). The lower boundary of the computational domain y=0 (XZ) is located on the surface of the Sun (photosphere) and contains the active region; the Y axis is directed from the Sun perpendicular to the photosphere. The X axis is directed from east to west, and the Z axis is from north to south. A typical magnetic field strength in the active region, $B_0 = 300$ G, was used as the unit of the magnetic field. In this domain, the complete magnetohydrodynamics system for compressible plasma with all dissipative terms was solved :

$$\frac{\partial \mathbf{B}}{\partial t} = \text{ rot } (\mathbf{V} \times \mathbf{B}) - \frac{1}{\text{Re}_m} \text{ rot } (\frac{\sigma_0}{\sigma} \text{ rot } \mathbf{B}) - \text{ rot } (\nu_{m\_Art} \text{ rot } \mathbf{B}) \quad (1)$$

$$\frac{\partial \rho}{\partial t} = - \text{ div } (\mathbf{V}\rho) \quad (2)$$

$$\frac{\partial \mathbf{V}}{\partial t} = -(\mathbf{V}, \nabla)\mathbf{V} - \frac{\beta}{2\rho}\nabla(\rho T) - \frac{1}{\rho}(\mathbf{B} \times \text{rot } \mathbf{B}) + \frac{1}{\text{Re}\rho}\Delta\mathbf{V} + $$
$$+ G_g\mathbf{G} + \nu_{Art}\Delta\mathbf{V} \quad (3)$$

$$\frac{\partial T}{\partial t} = -(\mathbf{V}, \nabla)T - (\gamma - 1)T \text{ div } \mathbf{V} + (\gamma - 1)\frac{2\sigma_0}{\text{Re}_m\sigma\beta\rho}(\text{ rot } \mathbf{B})^2 -$$
$$-(\gamma - 1)G_q L'(T)\rho + \frac{\gamma - 1}{\rho} \text{ div } [\mathbf{e}_\parallel \kappa_{dl}(\mathbf{e}_\parallel, \nabla T) +$$
$$+ \mathbf{e}_{\perp 1}\kappa_{\perp dl}(\mathbf{e}_{\perp 1}, \nabla T) + \mathbf{e}_{\perp 2}\kappa_{\perp dl}(\mathbf{e}_{\perp 2}, \nabla T)] \quad (4)$$

(details in [6, 16, 17])

Important parameters of the MHD equations are the magnetic Reynolds number Re_m and the ordinary Reynolds number Re, which determine the predominance of the transfer of the magnetic field and matter over the diffusion spreading due to magnetic viscosity and ordinary viscosity were choosen according to principle of limited simulation [19] ($Re_m = 3 \times 10^4, Re = 10^4$) .

In order to determine the evolution of the magnetic field in corona by solving the equations of magnetic hydrodynamic (1-4), it is necessary to know the magnetic field in the corona at the initial moment of time and the magnetic field on the photosphere during the time interval of calculation.

The initial magnetic field is taken to be a potential magnetic field that should approximate the corona field well enough at the initial time several days before the flares occur, when there are no strong disturbances. To set the conditions at the photospheric boundary, it is necessary to know two magnetic field components parallel to the boundary. This is because the magnetic field component normal to the boundary is found from the condition div $\mathbf{B} = 0$, and in the case of using a finite-difference scheme conservative with respect to the magnetic flux, the normal field component is calculated automatically when solving the MHD equations. During the calculated time period, regular distributions of the magnetic field vector have not yet been observed, so the field components necessary for setting the boundary conditions were found from the calculated potential field. This approximation can be used because the magnetic field on the photosphere is determined mainly by currents beneath the photosphere, not in the corona. To determine the potential field in the

corona, it is necessary to solve the Laplace equation for the magnetic field potential with the oblique derivative along the line of sight as a boundary condition. The oblique derivative along the line of sight of the magnetic field potential, specified at the boundary, is expressed through the component of the magnetic field along the line of sight. The line-of-sight photospheric magnetic field distribution B_{lsight} was taken from the SOHO MDI magnetic field maps (http://soi.stanford.edu/magnetic/index5.html). The setting of the problem, which was solved numerically, is as follows:

$$\Delta\varphi = 0; \quad \left.\frac{\partial\varphi}{\partial l_{sight}}\right|_{PhBoun} = -B_{sight}; \quad \mathbf{B} = -\nabla\varphi \tag{5}$$

For the numerical solution of MHD equations, the absolutely implicit upwind finite-difference scheme, conservative relative the magnetic flux, has been developed [6, 16]. The scheme is solved by the method of iterations. Special methods were developed with the aim of constructing a scheme that remains stable for the maximum possible time step. The scheme was realized in the computer program PERESVET.

The Laplace equation for the magnetic field potential with the oblique derivative (5) to find potential magnetic field is solved by two methods using a finite-difference scheme. In the first of them simple iterations are used, in which the values of the potential in the central point of a stencil is found via the neighboring points at the previous iteration. The second method consists in relaxation of the evolutionary diffusion equation

$$\frac{\partial\varphi}{\partial t} = D\Delta\varphi \tag{6}$$

During solving by the first method the iterations are converged slowly, because the operator of passing from the previous iteration to the current one is weakly contraction operator, e. g. its norm is not much less than unit. Such a method of solving is used in the first turn for checking. The solution obtained by this method is coincided with the solution obtained by the second method. The implicit scheme is used for diffusion equation (6) solving. This scheme is solved by an iteration method at the each time step. To accelerate the calculation a special algorithm is developed, according to which the small number of iteration is performed at first time steps, and further the number of iterations are gradually increased. Decrease of calculation time is achieved due to the diminishing the solution precision of the diffusion equation (6). But the solution precision of the Laplace equation (5), to which the solution of diffusion equation is tended for $t \to \infty$, does not become worse.

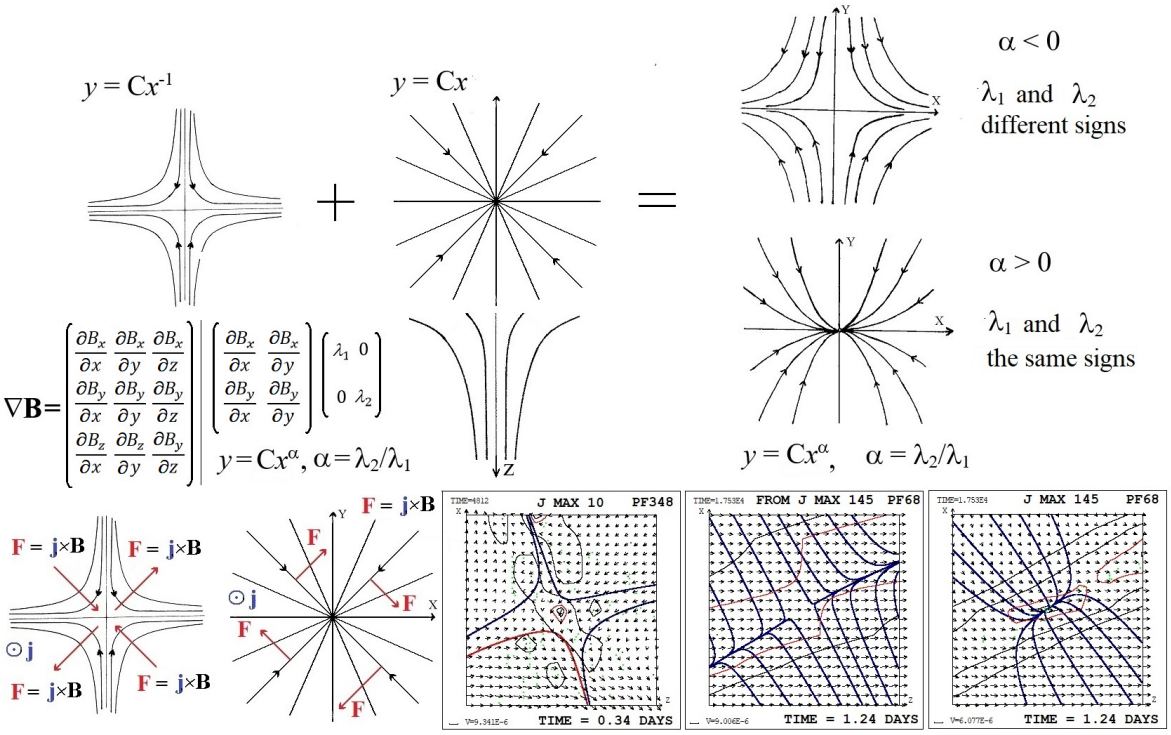

Figure 1. Overlay of a diverging magnetic field on an X-type field in the vicinity of a singular line.

Parallelization of calculations was carried out by computational threads on modern graphics cards (GPU) V-100 and Titan-100 using CUDA technology.

For small magnetic and usual viscosities, numerical instabilities arose near the boundary of the computational domain, which were stabilized using the developed methods [6].

The magnetic field configuration obtained by MHD simulation is so complex that it is often impossible to determine the positions of special lines and the current sheets appearing near them. For this purpose, a graphical search system [18] was developed, based on determining the positions of the current density maxima, which are achieved in the centers of the current sheets. The current density maxima are located on singular lines of the magnetic field.

3. MAGNETIC FIELD CONFIGURATIONS NEAR THE FOUND SINGULAR LINES AND CURRENT SHEETS

In the vicinity of an X-type singular line, the current directed along the singular line creates forces $\mathbf{j}\times\mathbf{B}$ directed toward the singular line along one direction (e.g., along the Y axis) and directed away from the singular line along another perpendicular direction (e.g.,

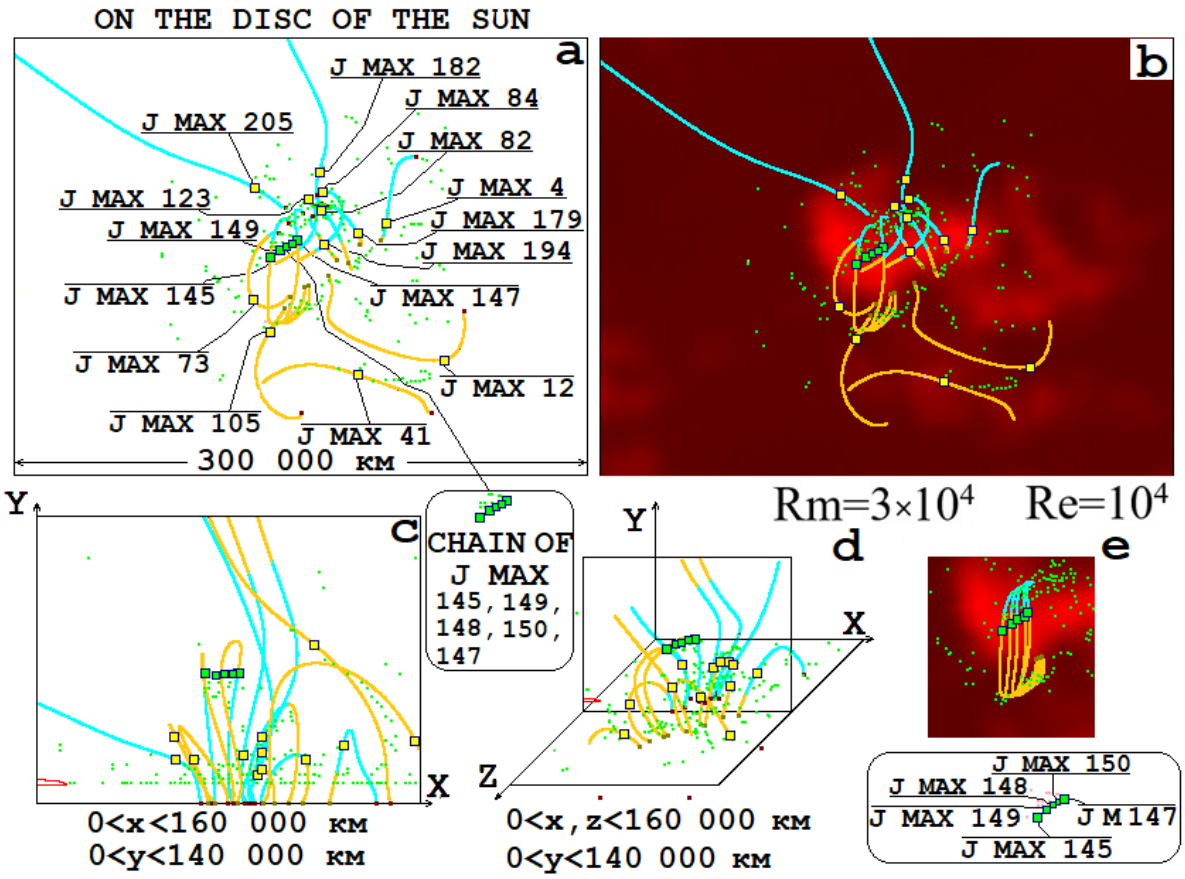

Figure 2. Positions of current density maxima in the computation domain of the corona in space, and their projections onto the central plane of the computation domain and onto the picture plane (perpendicular to the line of sight). The magnetic field configuration is represented by magnetic lines passing through selected current density maxima and their projections onto planes. Projections of magnetic lines onto the picture plane (a). The distribution of microwave radio emission at a frequency of 17 GHz, obtained on the solar disk using the Nobeyama radioheliograph, is superimposed on the picture plane with projections of magnetic lines (b). Magnetic lines in three-dimensional space (c) and their projections onto the central plane of the computation domain of the corona. The chain of maxima consists of points marked in green. The projections of magnetic lines passing through the maxima of this chain onto the picture plane are shown separately in an enlarged scale (e). Magnetic lines in front of the central plane of the computation domain of the corona are shown in light brown, and behind the central plane are shown in light blue.

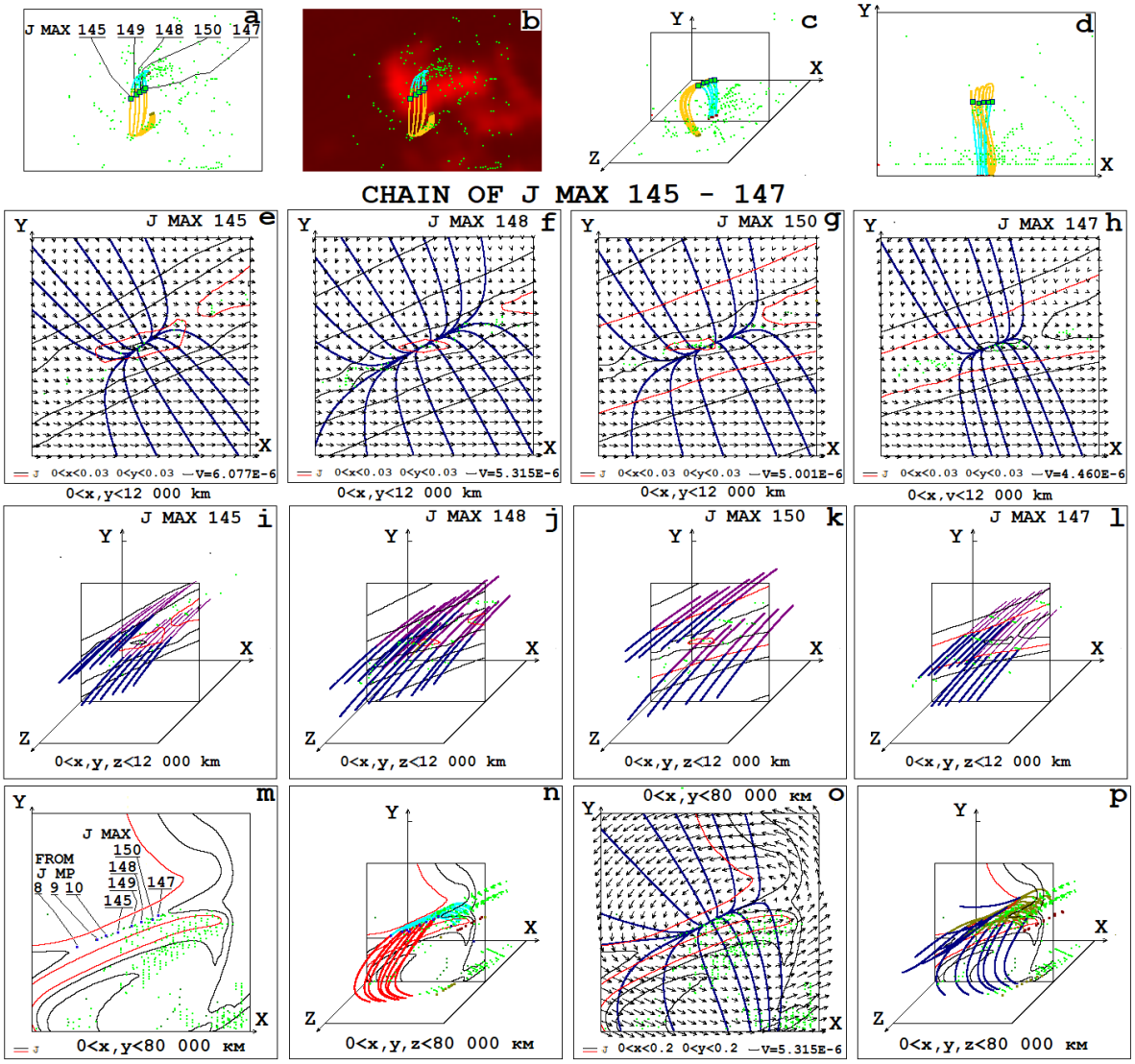

Figure 3. Magnetic lines passing through the points of the selected chain of current density maxima (a-d). Plane (e-h) and spatial (i-l) configurations in regions of 12,000 km in size with centers at the points of the chain of maxima. Plane (m, o) and spatial (n, p) configurations in large region of 80,000 km in size with center at the central maximum of the chain.

along the X axis). These forces create a plasma flow that deforms the magnetic field into a configuration corresponding to the current sheet. During the formation of the current sheet, the current density **j** , and therefore the force **j**×**B** , increases. Since the current **j** is created by disturbances in the plasma with a magnetic field propagating from the solar surface, in fact, in the vicinity of the X-type singular line, there is an accumulation of disturbances with the formation of a current sheet.

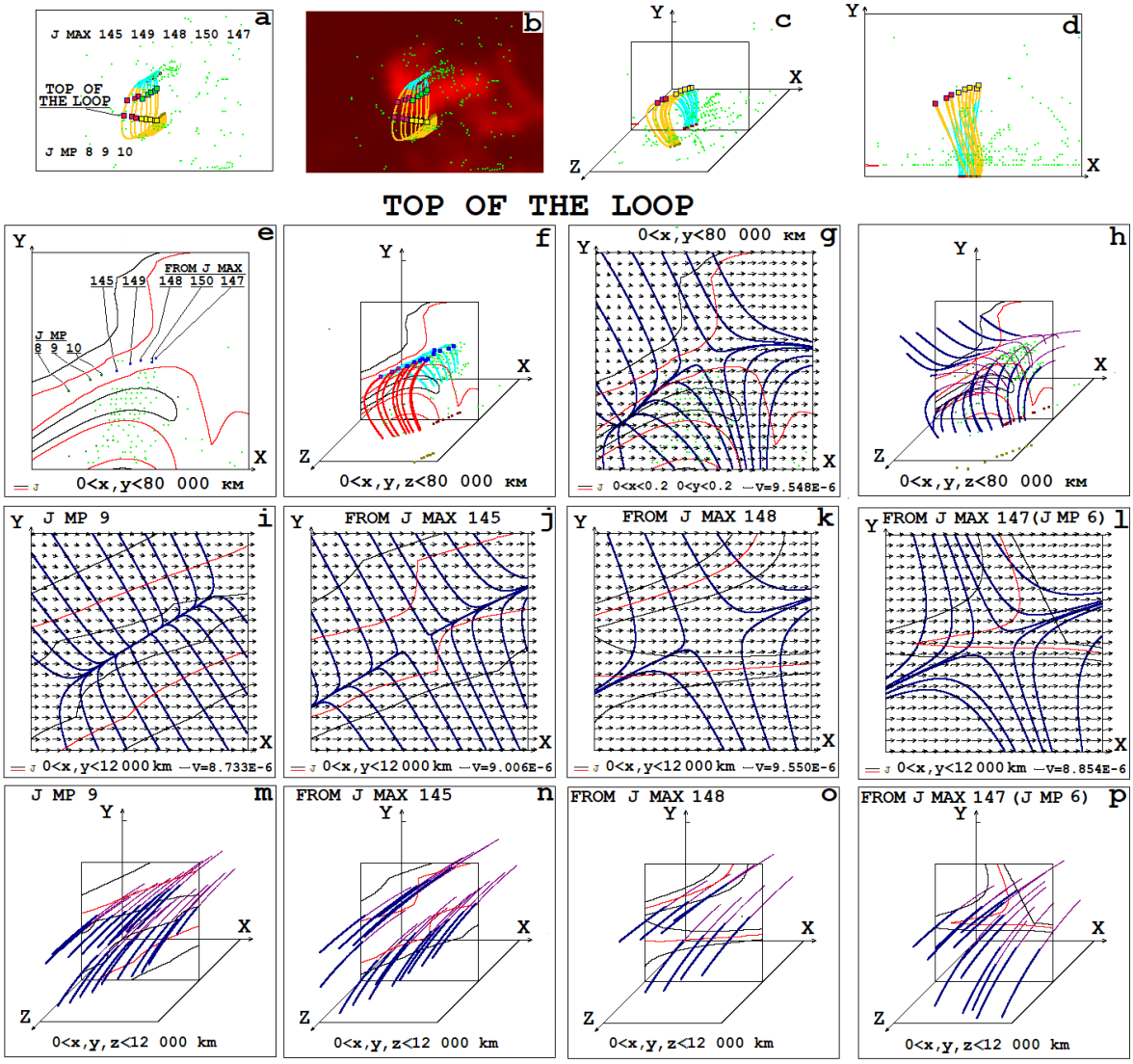

Figure 4. Magnetic lines passing through the maxima of the chain and magnetic lines passing through the flat maxima at the apex of the arc (a-d). Current density maxima are marked in green, and the points on the lines passing through them at the top of the arc are marked in yellow. Plane maxima at the top of the arc and the points of intersection of the lines passing through them with the plane passing through the central maximum of the chain J MAX 148 perpendicular to the magnetic field vector at this point are marked in red. Plane (e, g) and spatial (f, h) configurations in large regions of 80,000 km with the center at the top of arcade on the line passing through central maximum of the chain. In the central plane of large size (e) are marked the plane maxima of the current density through which the selected magnetic lines of the arch (f) pass, and the points of intersection of the lines of the arch passing through the maxima of the chain with this central plane. On this central plane (e) are depicted the lines of equal current density. Plane (i-l) and spatial (m-p) configurations in areas of 12,000 km with centers on the top of arcade.

Magnetic forces $\mathbf{j}\times\mathbf{B}$, creating plasma flows that deform the field into a current sheet configuration, lie in a plane perpendicular to the singular line and are determined by the current component along the singular line and the magnetic field components in the plane perpendicular to the singular line (perpendicular to the direction of the main current). Therefore, the main role in the formation of current sheets is played by plane magnetic field configurations represented by "plane magnetic lines", i.e. lines tangent to the projections of the magnetic field vectors onto the plane perpendicular to the singular line (we will call this plane the current sheet configuration plane, since it is in this plane that the plasma flow caused by $\mathbf{j}\times\mathbf{B}$ forces creates the current sheet and in this plane the current sheet field configuration is most clearly expressed).

The view of the three-dimensional configuration of the magnetic field can be used to determine to what extent the conditions determined by the longitudinal (directed along the singular line) component of the magnetic field contribute to the occurrence of a flare. The more the magnetic lines diverge in three-dimensional space along the singular line, the more favorable the conditions are for the occurrence of a solar flare, since the smaller the longitudinal magnetic field, which prevents the formation of a current sheet and the development of flare instability (the pressure forces of the longitudinal component of the magnetic field, as well as the gas-dynamic pressure forces, which have the same direction, are directed against the forces $\mathbf{j}\times\mathbf{B}$, which create a current sheet, and then instability of the current sheet).

In general, in the vicinity of a singular line, a field that diverges in a plane perpendicular to the singular line (in the plane of the current sheet configuration) can be superimposed on the X-type magnetic field configuration (see Fig. 1). The superposition results in a deformed X-type field if the X-type field dominates, or a deformed diverging magnetic field if the diverging field dominates. Since the divergence of the magnetic field in the plane is nonzero, to satisfy the condition $\mathrm{div}\ \mathbf{B} = 0$, it is necessary the changing the longitudinal component along the singular line ($\partial B_z/\partial z \neq 0$, here the Z axis is directed along the singular line), i.e. the configuration becomes essentially three-dimensional. The arrangement of the magnetic field lines in the direction of the Z axis is shown in Fig. 1 under the image of the diverging magnetic field. Such a field appears in magnetic traps of the mirror cell type in plasma installations created to solve the problem of controlled thermonuclear fusion. The dominance of the X-type field or divergent magnetic field is determined by the signs of the eigenvalues

of the matrix $\nabla\mathbf{B}$ (Fig. 1). In this case, these are the eigenvalues of the 2×2 matrix for the coordinates of the XY plane perpendicular to the singular line. For an ideal singular line, this matrix is diagonal, since $\partial B_x/\partial z = \partial B_y/\partial z = \partial B_z/\partial x = \partial B_z/\partial y = 0$. As calculations have shown, in the locations of current density maxima found by the graphical system for searching for flare positions, the values of $\partial B_x/\partial z, \partial B_y/\partial z, \partial B_z/\partial x, \partial B_z/\partial y$ are small compared to the elements of a 2×2 diagonal matrix $(\partial B_x/\partial x, \partial B_x/\partial y, \partial B_y/\partial z, \partial B_y/\partial y)$ and therefore the processes associated with them will not have a significant effect on the accumulation of disturbances with the formation of a current sheet determined by the elements of a 2×2 diagonal matrix.

Examples of superpositions of the X-type magnetic field and the divergent magnetic field obtained as a result of MHD modeling above the active region are shown in the lower right corner of Figure 1. The cases shown are those in which the X-type field predominates, the divergent magnetic field predominates, and both types of fields have almost equal influence.

The diverging magnetic field causes plasma rotation around a singular line, hindering the formation of a current sheet and the appearance of flare instability in the formed current sheet. Therefore, the predominance of the X-type configuration is a more favorable condition for the occurrence of a solar flare.

4. RESULTS OF MHD SIMULATION: EXTENDED SURFACE OF MAGNETIC LINES PASSING THROUGH THE CHAIN OF CURRENT DENSITY MAXIMA

The detailed study of the preflare situation at 02:32:05 on May 26, 2003 three hours before the flare M 1.9 is performed by comparing the results of MHD simulation above the active region AR 10365 with observations of microwave radio emission at 17 GHz obtained from the Nobeyama Radioheliograph (NoRH). In this moment the energy for solar flare is accumulated in the magnetic field and plasma of solar corona is heated by currents which creates this magnetic field. Magnetic field configuration is s represented by lines passing through maxima of current density with the numbers 145, 147, 194, 179, 4, 73, 105, 41, 12, 205, 123, 82, 84, 182 (Fig. 2.).

The intensity distribution of microwave radiation at a frequency of 17 GHz observed on the solar disk using the Nobeyama radiheliograph (NoRH) is superimposed on the projections of magnetic lines (Fig. 2a) onto the picture plane perpendicular to the line of sight (Fig. 2b).

3D magnetic lines in the computational domain in the corona (Fig. 2c), and projections of magnetic lines (Fig. 2d) onto the central plane of the computational domain (plane passing through the center of the computational domain, located parallel to the solar equator and perpendicular to the solar surface) are shown.

Magnetic field configurations at selected current density maxima points indicate promotable conditions for flare occurrence at some maxima located in the region of bright flare emission. There is no significant dominance of the diverging magnetic field in the vicinity of these maxima. At the same time, maxima with such properties also occur outside the bright region of flare emission, and there are not many such maxima in the bright region compared to their total number.

The problem of coincidence of bright flare emission regions with flare positions found from MHD simulation results can be solved by the occurrence of the surface of high current density, the current passing through a chain of current density maxima. The maxima of this chain with numbers 145, 149, 148, 150 and 147 in Figure 2 are shown by green dots. Magnetic lines on the solar disk passing through the maxima of this chain are shown separately on an enlarged scale. (Fig. 2e)

Figures 3a-d show magnetic lines in the computation domain of the corona, passing through the maxima of the selected chain. Their projections on the picture plane (Fig. 3a, b), location in three-dimensional space in the calculated region of the corona (Fig. 3c), and projections on the central plane of the calculated region (Fig. 3d) are presented. Also Figure 3 shows the plane (Fig. 3e-f) and three-dimensional (Fig. 3i-l) configurations near the chain maxima in a square and in a cube of 12,000 km. The two-dimensional region is a square of 12,000 km in size with the center at the point of the selected current density maximum, with the plane of the square located perpendicular to the magnetic field vector at the point of the selected maximum (perpendicular to the magnetic line passing through the point of the selected maximum). The three-dimensional region is a cube 12,000 km in size centered at the point of the selected maximum of current density, so that the two-dimensional region is the central plane of this cube, i.e. a plane passing through the center of the cube parallel to two faces of the cube and, accordingly, perpendicular to the other four faces of the cube.

These configurations do not have properties that could significantly promote the flare release of energy. In plane configurations, the divergent magnetic field dominates over the X-type field, although not very strongly, and in three-dimensional configurations, the field lines

do not diverge much along the singular line, which means a comparatively large longitudinal component of the magnetic field stabilizing the explosive instability.

The chain maxima are located close to each other (Fig. 3a-d) and the field configurations in their vicinity are very similar (Fig. 3e-f ш Fig. 3i-l), so that an assumption arises that all the chain maxima belong to the same current sheet of considerable width (50,000 km), i.e. an extended surface with an increased current density. This assumption is confirmed by the study of plane and three-dimensional configurations in a square and in a cube with a larger size of 80,000 km with the center at the 148th maximum located in the middle of the chain (Fig. 3m-p). The square is the central plane of the cube. In the square of a large size the intersection points of the magnetic lines passing through the chain maxima with the plane and also lines of equal current density are shown (Fig. 3m). Magnetic lines in a cube passing through the chain maxima form an arcade (Fig. 3n). The plane and three-dimensional configurations in large areas are shown in Figures 3o, p.

The current density maxima are not located at the loop top. It is necessary to construct a magnetic configuration at the top of the loop, where, from general considerations about the field configuration with sources under the solar surface, there should be practically no diverging field superimposed on the X-type field, and where, judging by the available observations, solar flares most likely occur. Such a construction is also necessary to check the coincidence of the surface of magnetic lines passing through the chain of current density maxima with the surface of increased current density.

In Figures 4a-d, the points lying on the loop apexes are marked in yellow, and the chain maximum points are marked in green (Fig. 4a,b). The points at the top of arcade are obtained as follows. On the magnetic line passing through the central maximum of the chain with the number 148, a point is sought at which the magnetic field vector is parallel to the solar surface (the component of the vector perpendicular to the solar surface is zero). This is the point at the top of the loop on the central line. A large area of 80,000 km is constructed with the center at this point. The plane of the square with the center at this point is perpendicular to the magnetic vector and is the central plane of the large cube.

The points on the solar disk and in the calculated region of the corona at the loop tops, marked in yellow (Fig. 4a-d), are the intersection points of the magnetic lines passing through the chain maxima with the constructed central plane. These points, designated as FROM J MAX 145, 149, 148, 150, 147, lie in the region of increased current density (Fig.

4e, which also shows the current density level lines), which confirms the coincidence of the surface of the lines passing through the chain maxima with the surface of increased current density. Plane maxima of J MP 8, 9, 10, which do not coincide with these intersection points of FROM J MAX (some flat maxima coincide with the points of FROM J MAX), are also designated on this plane (Fig. 4e). In the upper rows of Figures 4a, b, in the picture plane on the solar disk and in the computational region, the points of these flat maxima are marked in red, and magnetic lines are drawn through them. The intersection points of these lines with the central plane of the chain of maxima are also marked in red in the upper part of Figures 4a, b. These eight lines, five of which pass through the maxima of the chain and three through the flat maxima of the current density, represent an arcade, which is depicted in a large cube (80,000 km) with the center at the point at the top of the arcade (Fig. 4f).

The magnetic field configurations (Fig. 4g, h) in the region of large size have properties that promote the development of flare instability. In the plane configuration, the X-type magnetic field dominates the divergent field (Fig. 4g), and in the three-dimensional configuration, the field lines diverge significantly in the direction along the singular line (Fig. 4h). The latter means that the longitudinal component of the magnetic field is relatively weak, so that it cannot stabilize the flare instability.

Comparison of two-dimensional and three-dimensional configurations in large regions of 80,000 km in size for the points of the chain of maxima and the points at the top of the arcade (Fig. 3o, p ш Fig. 4g, h) shows a much more promotable situation for the occurrence of flare instability at the loop tops, rather than at the points of the chain maxima. The same result is obtained by comparing the magnetic field configurations in small regions (12,000 km in size) at the location of the chain of maxima (Fig. 3e-h and Fig. 3i-l) and at the top of the arch (Fig. 4i-l and Fig. 4m-p).

5. DISCUSSION AND CONCLUSION

Thus, the occurrence of a surface of increased current density located on magnetic lines passing through a chain of current density maxima can solve the problem of coincidence regions of bright flare radiation with the positions of flares found from the results of MHD simulation using a graphical search system based on the search for current density maxima. During flares, the energy of the magnetic field of the current located on the surface of

increased current density can be released. This surface of increased current density is an arcade of magnetic lines passing through a chain of current density maxima. In fact, this surface is an extended current sheet.

The instability leading to the main energy release of the flare can begin at the top (or near the top) of the arcade, where current density maxima may not appear. However, the current density in this place is large enough, differing little from the current density in the maxima located far from the top of the arcade. Also, plane current density maxima can be located at the tops of the arcades, in a plane perpendicular to the magnetic vector. The reason for the appearance of flare instability at the top of the arcade is the properties of the magnetic field configuration in this place, which promote to the occurrence of instability of the current sheet (the dominance of the X-type field and the significant divergence of magnetic lines in three-dimensional space along the direction of the special line, which means a small value of the longitudinal component of the current sheet). Further, the instability can spread to the entire region of the current sheet, which is confirmed by the location of the entire arcade with an increased current density in the region of bright flare radiation.

The appearance of current density maxima with magnetic field configuration properties, that promote flare instability, outside the bright flare region can be explained by the location of these magnetic field features out of the powerful arcade with increased current density, due to which much energy will not accumulate in the resulting current sheet.

The proposed solution to the problem of the coincidence of the flare position found from the results of MHD simulation with the bright region of flare (or pre-flare) emission needs further verification. This verification should be carried out by carefully searching for all features of the magnetic field found by MHD simulation and comparing the position of these features with the position of the bright region for this moment and other moments of the selected flare and other flares.

ACKNOWLEDGMENTS

The authors are grateful to the SOHO/MDI (Michelson Doppler Imager on the spacecraft Solar and Heliospheric Observatory) team and the Nobeyama radioheliograph team (The Nobeyama Radio Observatory, the division of the National Astronomical Observatory of Japan, located near Minamimaki, Nagano at an elevation of 1350 m.) for the scientific data

provided as well as to the many professional cloud service specialists who made it relatively easy for us to configure rented remote computers for GPU computing.

---

1. Lin, R.P.; Krucker, S.; Hurford, G.J.; et al. RHESSI observations of particle acceleration and energy release in an intense solar gamma-ray line flare. Astrophys. J. 2003, **595**, L69-L76.
2. Podgorny, A.I., Podgorny, I.M.„ Meshalkina, N.S. Dynamics of magnetic fields of active regions in pre-flare states and during solar flares. Astron. Rep. 2015, **59**(8), 795-805.
3. Podgorny, I.M.; Podgorny, A.I. Diagnostic of a solar flare via analyses of emission in spectral lines of highly ionized iron. Astron. Rep. 2018, **62**(10), 696-704.
4. Podgorny I.M., Podgorny A.I. X8.2 Solar flare on the rear side of the solar disk: An evidence for the current sheet as a mechanism for cosmic ray acceleration. Sun and Geosphere, 2019, **14**(1), 13-19.
5. Podgorny, A.I., Podgorny, I.M. Formation of Several Current Sheets Preceding a Series of Flares above the Active Region AR 0365. Astronomy Reports, 2008, **52**(8), 666-675
6. Podgorny, A.I., Podgorny, I.M., Borisenko, A.V. MHD Simulations of the Solar Corona to Determine the Conditions for Large Solar Flares and the Acceleration of Cosmic Rays during Them. Physics 2023, **5**(3), P. 895-910.
7. Jiang, C., Wu, S.T., Yurchyshyn, V. et al. How did a major confined flare occur in super solar active region 12192? Astrophys. J. 2016, 828:62, 12(pp).
8. Syrovatskii, S.I. Dynamic dissipation of energy in the vicinity of the magnetic field neutral line. Sov. Phys. JETP 1966, **23**, 754-762.
9. Bratenahl, A., Hirsch,W. An experimental study of a neutral point in a plasma. In Proceedings of the AIAA Plasma dynamics Conference, Monterey, CA, USA, 2-4 March 1966; pp. 66-152.
10. Podgorny, I.M., Balabin, Y.V., Vashenyuk, E.V., Podgorny, A.I. The generation of hard X-rays and relativistic protons observed during solar flares. Astron. Rep. 2010, **54**(7), 645-656.
11. Podgorny, I.M., Dubinin, E.M., Israilevich, P.L., Nicolaeva, N.S. Large-scale structure of the electric field and field-aligned currents in the auroral oval from the Intercosmos-Bulgaria satellite data. Geophys. Res. Lett. 1988, **15**(13), 1538-1540.
12. Podgorny, A.I., Podgorny, I.M. Acceleration of Solar Cosmic Rays in a Flare Current Sheet and Their Propagation in Interplanetary Space. Astron. Rep, 2015, **59**(9), 888-897

13. Podgorny I.M., Podgorny A.I. Proton acceleration in the solar flare. J. Atmosph. Solar Terrestr. Phys., 2018, **180**, 9-15
14. Podgorny, I.M.; Kovalskii, N.G.; Pal'chikov, V.E. Electrons that produce the hard X-ray radiation of powerful pulsed discharges. Sov. Phys. Doklady 1958, **3**, 1208-1211
15. Podgorny, I.M.; Balabin, Y.V.; Podgorny, A.I.; Vashenyuk, E.V. Spectrum of solar flare protons. J. Atmos. Sol. Terr. Phys. 2010, **72**, 988-991
16. Podgorny, A.I., Podgorny, I.M. MHD simulation of phenomena in the solar corona by using an absolutely implicit scheme. Comput. Math. Math. Phys. 2004, **44**(10), 1784-1806.
17. Podgorny A. I., Podgorny I. M., Meshalkina N. S. Current sheets in corona and X-ray sources for flares above the active region 10365. Journal of Atmospheric and Solar-Terrestrial Physics. 2018, **180**, 16-25
18. Podgorny A.I. and Podgorny I. M. MHD simulation of solar flare current sheet position and comparison with X-ray observations in active region NOAA 10365. Sun Geosph. 2013, **8**(2), 71-76.
19. Podgorny, I.M. Simulation studies of Space. Fundam. Cosm. Phys. 1978, **4**, 1-72.